direction, the transverse dispersion curves T_2 in the [$\zeta\zeta$0] direction, and the longitudinal and transverse dispersion curves in the [$\zeta\zeta\zeta$] direction are identical for the two angular-force models. Figure 1(a) and 1(b) of this paper and Figs. 3(a) and 3(b) of Ref. 1 show that for the remaining three branches the curves from the DAF model are in poorer agreement with the experimental data than those from the CGW model.

The frequency spectrum for the DAF model, while showing two peaks as in the case of CGW model, gives a somewhat greater weight to the low-frequency peak as compared with the spectrum obtained from the CGW model.

The theoretical curve for Θ_D lies below the experimental points over the whole temperature range. The curve shown in Fig. 3 was obtained from the 0°K frequency-spectrum histogram. If calculations are carried out in the quasiharmonic approximation, the theoretical curve is found to be lower than that shown in Fig. 3, i.e., the divergence from the experimental data is greater.

Further, note that the DAF model suffers from the defect of not being rotationally invariant. The CGW model, on the other hand, is rotationally invariant.[11]

In conclusion, we find that for copper the CGW model is better than the DAF model.

ACKNOWLEDGMENTS

The authors are grateful to Dr. J. A. Morrison for helpful discussions and to the National Research Council of Canada for financial support.

[11] D. C. Gazis and R. F. Wallis, Phys. Rev. **151**, 578 (1966); **156**, 1038 (1967).

PHYSICAL REVIEW VOLUME 174, NUMBER 3 15 OCTOBER 1968

Optimum Form of a Modified Heine-Abarenkov Model Potential for the Theory of Simple Metals*

ROBERT W. SHAW, JR.†
Division of Applied Physics, Stanford University, Stanford, California 94305
(Received 1 March 1968)

A modified form of the Heine-Abarenkov model potential is proposed. The core potential is replaced with a constant potential A_l only for those angular momenta for which there are core wave functions. Also, the model radius R_l is allowed to be different for each l and to depend on energy. It is shown that this potential can be optimized using a variational procedure. The optimum model parameters are obtained by choosing an R_l such that $A_l=-v(R_l)$. The optimized form of this modified model potential has several advantages. It provides a unique prescription for selecting model radii, and it eliminates the necessity of approximating the A_l for $l>2$. Also, the form factors tend to decay rather than oscillate at short wavelengths. The linear extrapolation of A_l versus E proposed by Animalu is shown to be valid for most simple metals. Optimum model potential parameters are obtained, and form factors and depletion holes are evaluated for a group of simple metals using the optimized model potential.

1. INTRODUCTION

THE Heine-Abarenkov (HA) model-potential theory[1–3] is, in a sense, a cross between the quantum-defect method[4] (QDM) and the pseudopotential method.[5] As in the pseudopotential method, the deep potential at each ion center is replaced with a shallow potential which is chosen so that the valence-electron wave functions have no nodes within the core. The actual value of the model potential, chosen for convenience to be a constant A_l for each value of angular momentum l, is determined in the spirit of QDM. One chooses a radius R_M outside the core and then adjusts A_l until the logarithmic derivative of the wave function inside R_M precisely matches the logarithmic derivative of the Coulomb wave function outside R_M. This matching is done only at the free-ion-term values, since only for these energies can we evaluate the external wave function without knowing the core potential (it is the Coulomb wave function that decays at infinity).

There are several features of this procedure that have never been adequately discussed. First, a single value of R_M is chosen for all l. This is not a necessary restriction but was made largely for simplicity. The choice of R_M for each element seems to have been somewhat arbitrary. Heine and Animalu[6] did notice that if they selected $A_l \cong Z/R_M$, the magnitude of the form-factor oscillations at short wavelength (large q) was reduced. Aside from this observation, no criterion has ever been given for the choice of model radius.

* Work supported by the Advanced Research Projects Agency through the Center for Materials Research at Stanford University.
† NASA trainee.
[1] V. Heine and I. V. Abarenkov, Phil. Mag. **9**, 451 (1964).
[2] I. V. Abarenkov and V. Heine, Phil. Mag. **12**, 529 (1965).
[3] A. O. E. Animalu and V. Heine, Phil. Mag. **12**, 1249 (1965).
[4] F. S. Ham, in *Solid State Physics*, edited by F. Seitz and D. Turnbull (Academic Press Inc., New York, 1964), Vol. 1, p. 127.
[5] W. A. Harrison, *Pseudopotentials in the Theory of Metals* (W. A. Benjamin, Inc., New York, 1966).

[6] A. O. E. Animalu and V. Heine (Ref. 3), Sec. 4.

Second, all the A_l for $l>2$ were set arbitrarily equal to A_2. The reason for doing this is that there are essentially no term values available for $l>2$, and therefore no direct way of calculating the A_l for these l's. The choice made by HA is convenient because it allows the potential to be collapsed from

$$w_0=-\sum_{l=0}^{\infty} A_l(E)P_l, \quad r<R_M$$

$$P_l=\sum_{m=-l}^{l} |Y_l^m\rangle\langle Y_l^m| \tag{1.1}$$

to

$$w_0=-(A_0-A_2)P_0-(A_1-A_2)P_1-A_2, \quad r<R_M. \tag{1.2}$$

However, it is clear that this choice of A_l means that the $l>2$ components of the model wave function cannot have logarithmic derivatives that match those of the true wave function at $r=R_M$. Also, it is not obvious precisely what the approximation means or whether anything important has been neglected. Though Heine and Abarenkov[7] have given several arguments in defense of their choice, it would improve the theory to eliminate this approximation.

The procedure outlined above gives values of A_l ($l=0, 1, 2$) for ionic-term values. To find A_l at an arbitrary energy, in particular at the Fermi energy of a metal composed of these model ions, it is necessary to make an extrapolation (see Figs. 3 and 6). Since the A_l at term energies usually lie roughly on a straight line, a linear extrapolation was made. Animalu[8] has indicated that this choice was really a guess, made for lack of a better procedure, and was never investigated closely. In particular, for $l=1$ and 2 the extrapolation had to be made over a large energy range and seemed risky at best. As it turns out, we can show (see Sec. 2) that, except for some special cases, the linear-extrapolation scheme is satisfactory.

There is one final point worth mentioning. As we have already remarked, Heine and Animalu[3] found that the model-potential form factors had oscillating short-wavelength tails. They briefly discussed the possible significance of these oscillations, pointed out that they were due to the discontinuity in the potential at R_M, and proposed a damping factor to suppress them. However, no effort has been made to determine whether these oscillations can be reduced by constructing a model potential that is in some sense optimum.

The main objective of this paper is to propose a modified form of the model potential. This new form of the potential has several advantages. It lends itself readily to a variational optimization procedure. The condition for optimization gives us a direct way to determine model radii. Also, the potential is constructed so that the question of how to determine the A_l for $l>2$ never arises. Aside from eliminating these difficulties with the old theory, the optimum form of the modified potential has another important feature: It gives form factors that tend to decay rapidly at short wavelengths instead of oscillating.

[7] V. Heine and I. V. Abarenkov (Ref. 1), p. 454.
[8] A. O. E. Animalu (private communication).

2. CONSTRUCTION OF THE MODEL POTENTIAL

A. Free-Ion Model Potential

Before we discuss our proposals for modifying the HA model potential, it is appropriate to consider in some detail the procedure used to construct the potential. To begin, we consider the Schrödinger equation for a single valence electron moving in the deep potential of a free metallic ion, e.g., Al^{+3}. It is convenient for the free-ion problem to make a spherical separation of the Schrödinger equation. The radial equation for the true wave function $\psi_l(r)$ for angular momentum l is simply (we use atomic units throughout)

$$\frac{d^2\psi_l(r)}{dr^2}-\left[\frac{l(l+1)}{r^2}+2v(r)-2E\right]\psi_l(r)=0. \tag{2.1}$$

We make two assumptions at the outset. First, we assume that for r greater than some reasonably small core radius R_C, the free-ion potential $v(r)$ can be regarded as local and, specifically, Coulombic. The validity of this assumption has been discussed in detail by Ham.[4] Second, we ignore conduction-electron effects, at least for the present. Interactions between conduction electrons will be accounted for when we screen the potential self-consistently. Interactions between conduction electrons and core electrons are treated in the small-core approximation, and are included as an energy shift when we calculate metallic energies, e.g., the Fermi energy. To justify our treatment of valence-core interactions we appeal to band-structure calculations which require the same assumption that we have made. These calculations have given excellent agreement with band-gap measurements for semiconductors and Fermi-surface data for metals. On the basis of this agreement we conclude that this part of the small-core approximation is not unreasonable. It is important to emphasize that a corresponding treatment of valence-core interactions is required in pseudopotential theory as well. Later in this section, we shall discuss this and another application of the small-core approximation in more detail.

The fundamental objective of model- (or pseudo-) potential theory is to replace the deep ion-core potential with a shallow potential that preserves the valence-electron energies. The essential point is that this shallow model potential can be treated as a perturbation. The method proposed by Heine and Abarenkov was to replace $v(r)$ with a square well $A_l(E)$ inside some model

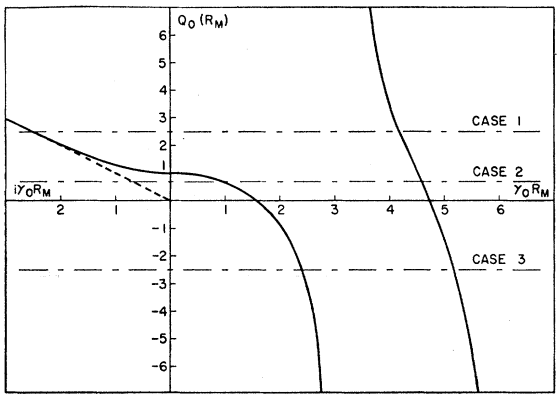

FIG. 1. The function $Q_l(R_M)$ for $l=0$ [defined in Eq. (2.4)]. The horizontal lines represent values for the logarithmic derivative of ψ_l for various combinations of R_M and E.

radius $R_M \gtrsim R_C$. The model Schrödinger equation is then

$$\frac{d^2\chi_l(r)}{dr^2}-\left[\frac{l(l+1)}{r^2}-\left(\frac{2A_l(E)}{2Z/r}\right)-2E\right]\chi_l(r)=0, \quad \begin{pmatrix} r<R_M \\ r>R_M \end{pmatrix}. \tag{2.2}$$

Note that from our first assumption $\chi_l(r)\equiv\psi_l(r)$ for $r>R_M$.

The $A_l(E)$ are determined in the spirit of QDM, that is, they are adjusted until the logarithmic derivatives of the internal and external solutions of (2.2) match at R_M. The external solution is uniquely defined only at free-ion-term values. At these energies a boundary condition at infinity can be imposed and the solutions become Whittaker functions of the first kind. In terms of the Wannier-Kuhn-Ham solutions,[4,9–11] we can write

$$\psi_l(r)\sim W_{n,l+1/2}\left(\frac{2Zr}{n}\right) = \frac{\Gamma(n+l+1)}{n^{l+1}}\tfrac{1}{2}zJ_{2l+1}{}^n(z)\cos(n-l-1)\pi + \Gamma(n-l)n^{l}\tfrac{1}{2}zN_{2l+1}{}^n(z)\sin(n-l-1)\pi, \tag{2.3}$$

where

$$z=(8Zr)^{1/2} \quad \text{and} \quad n=Z/|2E|^{1/2}.$$

The interior solutions of (2.2) are simply spherical Bessel functions; therefore the logarithmic-derivative matching condition is

$$Q_l\equiv\frac{\gamma_l R_M j_{l-1}(\gamma_l R_M)}{j_l(\gamma_l R_M)}-l=\left(\frac{r}{\psi_l}\frac{d\psi_l}{dr}\right)_{R_M}, \tag{2.4}$$

$$\gamma_l=[2(A_l+E)]^{1/2}.$$

[9] G. H. Wannier, Phys. Rev. **64**, 358 (1943).
[10] T. S. Kuhn, Quart. Appl. Math. **9**, 1 (1951).
[11] F. S. Ham, Quart. Appl. Math. **15**, 1 (1957).

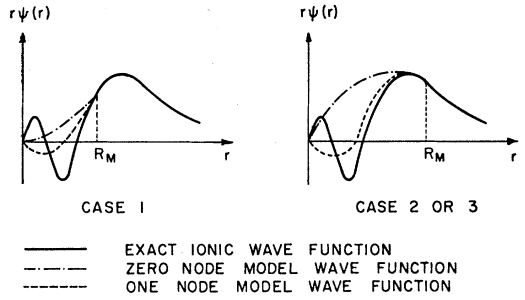

FIG. 2. Schematic examples of model wave functions for the possible matching conditions illustrated in Fig. 1.

Note that for $l=0$ we use $-n_0(\gamma_0 R_M)$ in place of $-_1(\gamma_0 R_M)$.] We have plotted the function Q_0 in Fig. 1. Since plots of all the other Q_l are similar, it is enough to concentrate on the $l=0$ case.

The procedure for obtaining A_l is, figuratively, to evaluate the right-hand side of (2.4), draw a horizontal line on the Q_l-versus-$\gamma_l R_M$ plot, and then determine A_l from the values of $\gamma_l R_M$ at the intersections. In Fig. 1, we have drawn lines corresponding to three possible cases for $l=0$. There are, of course, an infinite number of intersections for any given value of logarithmic derivative. Each corresponds to matching ψ_l to a model wave function with a different number of nodes in the core. We have shown the situation schematically in Fig. 2 for the cases indicated in Fig. 1.

We have emphasized that our aim is to replace the core potential with the weakest possible model potential in order that we be justified in using perturbation theory. Clearly, the weaker the potential, the fewer the number of nodes that the model wave function will have inside the core. It is therefore entirely within the spirit of our objective to choose, in each case, the $A_l(E)$ which corresponds to a nodeless model wave function. That is, we select the intersection with the first branch in a plot such as Fig. 1. [Note that if the intersection is on the imaginary γ_l branch, that is, $|E|>A_l$, then $\chi_l(r)$ is a decaying wave function within the core.] If the first branch of Q_l is used to determine $A_l(E)$ for all l, then each component $\chi_l(r)$ of the model wave function will be nodeless and the entire function

$$\chi_k(\mathbf{r})=\sum_{l,m}\frac{\chi_l(kr)}{r}Y_l{}^m(\vartheta,\varphi) \tag{2.5}$$

will be nodeless as well.

Abarenkov[12] has solved (2.4) by machine, using a method analogous to the graphical determination that we have discussed. In Fig. 3, we give a plot of Abarenkov's results for $ZR_M=4$ and $l=0$. To obtain the curve of $A_l(E)$ shown (solid line), Abarenkov assumed that each energy was a free-ion eigenvalue and used (2.3) to determine the external logarithmic derivative. The

[12] I. V. Abarenkov, Cavendish Laboratory Technical Report No. 2, Cambridge, England (unpublished).

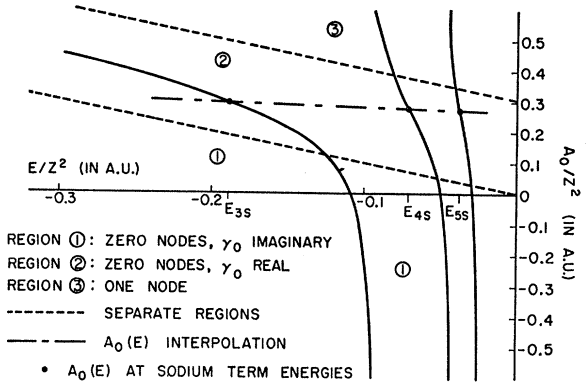

FIG. 3. A typical set of results from Abarenkov's tables of model potential parameters. The dashed lines divide the plot into regions corresponding to various numbers of nodes in the model wave functions. The model parameters at a typical set of s-term values E_1, E_2, and E_3 are shown. The dash-dot line indicates the linear interpolation-extrapolation procedure suggested by Animalu.

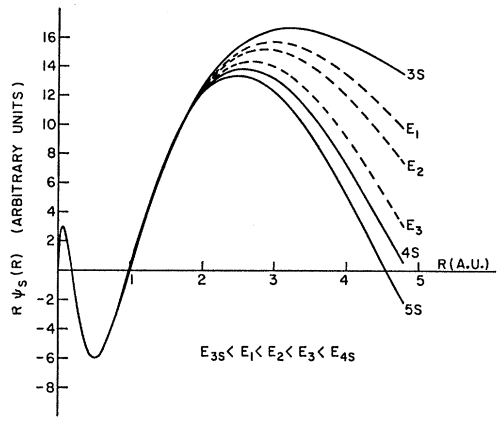

FIG. 4. Na^+ s wave functions calculated using a Hartree-Fock potential (Ref. 14). The dashed lines indicate wave functions with energies between E_{3s} and E_{4s}.

singularities occur at energies for which $\psi_l(r)$ has a node at $r=R_M$. Figure 3 has been divided into regions corresponding to various numbers of nodes by noting, from Fig. 1, that when

$$A_0=-E+\tfrac{1}{2}(\pi n/R_M)^2, \qquad (2.6)$$

the number of nodes in the matching solution increases from $n-1$ to n. A similar division can be made for any A_l-versus-E plot.

Using a plot such as Fig. 3, we can determine the value of A_0 at free-ion eigenvalues. A typical set of points is indicated on the figure. When we combine model ions to form a metal, it will be necessary to evaluate A_l at energies between or below the term values by interpolating or extrapolating. Animalu[8] found that for most simple metals the A_l at term values fell on a straight line, and he therefore extrapolated linearly (Fig. 3). Before we can use this procedure with confidence, we must provide some justification for it.

There are really two problems to consider. The first is whether the A_l at term values can be connected by a smooth line at all. If there were a singularity in the logarithmic derivative at R_M for some energy between terms, we would expect the solution on the first branch of Fig. 1 to jump abruptly from one end of the branch to the other. Such a jump would obviously preclude smooth interpolation. The second problem is, assuming that a linear connection between terms is valid, how far below the lowest term value can we safely extrapolate linearly?

These questions can be answered easily by studying wave functions. However, before we do that, we can make a general statement about the $A_l(E)$ curve by invoking the following theorem[13]:

Let $L(E,a)$ be the logarithmic derivative of a one-dimensional wave function at $r=a$ and energy E. Then, for $r>a$, $L(E,r)$ is a monotonically decreasing function of E [Ref. 13 includes functions such as $\cot(E)$ in the class of monotonic functions].

Since the logarithmic derivative of the true wave function $\psi_l(r)$ [defined as in (2.5)] is zero at $r=0$ for all l, it follows that at $r=R_M$ the logarithmic derivative must decrease with energy. In terms of our graphical discussion of the matching procedure, this means that the horizontal lines in Fig. 1 must move down as energy increases. Therefore, on a plot such as Fig. 3, the $A_l(E)$ curve can move only from a region with n nodes to one with $n+1$ nodes.

To show that linear interpolation of $A_l(E)$ between term values is extremely reasonable, we consider the s wave functions for Na^+ obtained using a self-consistent Hartree-Fock potential[14] (Fig. 4). For energies between eigenvalues the wave functions are, of course, singular at $r=\infty$, but for the range of r shown the wave functions at intermediate energies fall between the eigen-

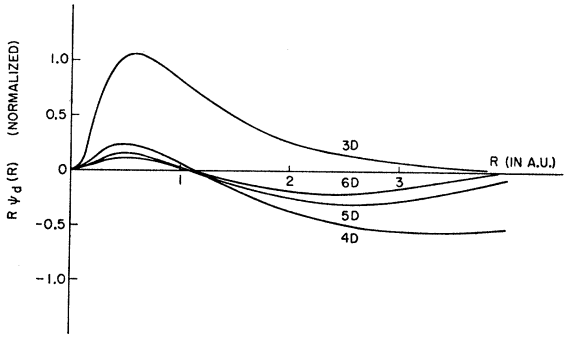

FIG. 5. Zn^{+2} d wave functions. The $3d$ wave function is from W. W. Piper, Phys. Rev. 123, 1281 (1961). The $4d$, $5d$, and $6d$ wave functions are from F. Herman (unpublished). The author is deeply grateful to Dr. Herman, who graciously offered to compute the Zn^{+2} d wave functions.

[13] A. Messiah, *Quantum Mechanics* (North-Holland Publishing Co., Amsterdam, 1961), p. 100.

[14] F. Herman and S. Skillman, *Atomic Structure Calculations* (Prentice-Hall, Inc., Englewood Cliffs, N. J., 1963).

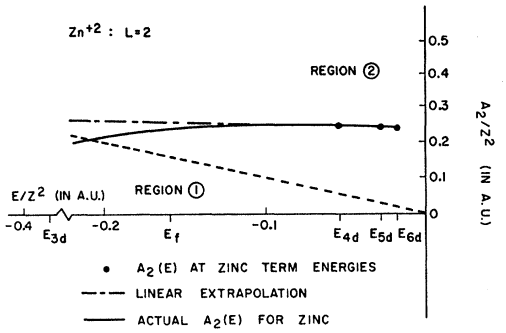

FIG. 6. Schematic $A_2(E)$ curve obtained from Zn^{+2} d wave functions. The linear extrapolation from ionic-term values is shown for comparison. The plot is divided into regions in the same manner as in Fig. 3.

functions. For Na^+ reasonable model radii are in the range $r=2$ to 4. For these radii the logarithmic derivative is clearly a smooth function of energy, and therefore $A_l(E)$ will be smooth. Though these considerations do not prove that linear interpolation is precisely correct, they indicate that it is at least not an unreasonable procedure, and is likely to be quite accurate.

Linear extrapolation to energies far below the lowest term value is not always justified. To illustrate the type of difficulties encountered, we consider the d states of Zn^{+2} (Fig. 5). The energy of the $3d$ core function is not far below the Fermi energy. Therefore for energies near E_F and for, say, $R_M=2$, the logarithmic derivative of the d functions is approaching a singularity. The actual $A_l(E)$ curve for this case is shown in Fig. 6. Clearly, a linear extrapolation to E_F is not correct. The d states of Zn^{+2}, Cd^{+2}, and Hg^{+2} are the only cases where the behavior shown in Fig. 6 is pronounced. Usually the highest core energy for a given l is far below the bottom of the conduction band and a linear extrapolation of $A_l(E)$ to E_F and below is an excellent approximation.

We conclude that, when the logarithmic derivative at R_M has no singularities in the range of energy in which $A_l(E)$ is to be determined, the linear interpolation or extrapolation procedure can be used with confidence. If there is any doubt, the results can be checked by actually computing wave functions numerically and evaluating $A_l(E)$ directly. The only cases among the simple metals where we have found difficulties in the linear procedure are the $l=2$ states of zinc, cadmium, and mercury. The reason for the difficulty is that the d bands in these materials are close to or within the free-electron-like band.

B. Model Potential in a Metal

The Schrödinger equation that describes a single conduction electron in a metal is

$$(T+\sum_i v_i+V_e)|\psi_k\rangle=E_k|\psi_k\rangle, \qquad (2.7)$$

where V_e is the self-consistent potential due to all the conduction electrons and the v_i are the ion-core potentials. One important feature of model-potential theory is that we do not require an explicit expression for v_i. We need only assume that v_i is Coulombic just outside the core. To construct a pseudopotential, however, we must know v_i inside the core and consequently must compute core wave functions explicitly and determine the exchange interaction between conduction and core states.

Now, suppose we consider the Schrödinger equation obtained by replacing all of the true ion potentials with model potentials w_i,

$$(T+\sum_i w_i+V_e)|\chi_k\rangle=E_k{}^M|\chi_k\rangle. \qquad (2.8)$$

The appropriate well depths for these potentials have yet to be determined. The same electron potential appears in this model equation as in (2.7). We have denoted the eigenvalue in (2.8) by $E_k{}^M$, since it is not immediately obvious that it should equal the true metallic eigenvalue E_k.

We confine our attention for the moment to a region around the jth ion. For this purpose it is convenient to rewrite (2.7) and (2.8) in the forms

$$(T+v_j)|\psi_k\rangle=(E_k-\sum_{i\neq j} v_i-V_e)|\psi_k\rangle \qquad (2.9)$$

and

$$(T+w_j)|\chi_k\rangle=(E_k{}^M-\sum_{i\neq j} v_j-V_e)|\chi_k\rangle. \qquad (2.10)$$

In (2.10), we have made use of the fact that outside of a given core $w=v$, that is, cores do not overlap. This assumption limits the method to metals in which the non-Coulombic part of the core potential is confined to a small region around the nucleus.

To proceed beyond this point it is necessary to make an additional small-core approximation. We assume that over the region of the jth core the potential $\sum_{i\neq j} v_i+V_e$ can be regarded as constant. It is this approximation that restricts application of the model-potential method to the simple metals. One can defend the approximation on the grounds that it is required in both the pseudopotential method and the QDM. However, that fact is essentially irrelevant. It is more important to realize that when cores overlap, the problem becomes sufficiently difficult that, as yet, no satisfactory model treatment has been given. For the present, we must restrict our attention to the simple metals for which the small-core approximation is reasonable. Harrison[5] has pointed out one way to assess the validity of the small-core approximation. He observed that the computed core wave functions for the free ion and free atom do not differ significantly and that the situation in the metal should be somewhere between these extremes. It is therefore clear that nothing of critical importance is being neglected.

We now define a new energy

$$E_k' = E_k - \sum_{i \neq j} v_i - V_e, \tag{2.11}$$

which we consider to be constant inside the jth core. Equations (2.9) and (2.10) then become

$$(T+v_j)|\psi_k\rangle = E_k'|\psi_k\rangle \tag{2.12}$$

and

$$(T+w_j)|\chi_k\rangle = (E_k'+E_k^M-E_k)|\chi_k\rangle \tag{2.13}$$

in this region. In our discussion of the free ion we found, in dealing with an equation identical to (2.12), that we could reproduce precisely the correct logarithmic derivative at a radius R_M by replacing (2.12) with a model equation inside the core. The appropriate model potential for arbitrary E was to be obtained by using the linear $A_l(E)$ relation. We use this prescription to determine w_j in (2.13), using $A_l(E_k')$ in the potential. It then follows immediately from (2.13) that $E_k^M = E_k$.

As a result of our assumption that E_k' is a constant, we have been able to construct a model potential for the metal. The logarithmic derivatives of $|\psi_k\rangle$ and $|\chi_k\rangle$ therefore match at model radii by construction. In addition, we find that the metallic eigenvalues are the same for the true and model problems. That this is true only in the small-core approximation illustrates an important difference between model-potential theory and pseudopotential theory in which the eigenvalues are equal by construction. We emphasize once more that the small-core approximation is an essential assumption of the theory. Without it we cannot construct a metal from model ions.

To actually determine the $A_l(E_k')$'s appropriate to a metal, we must calculate E_k' relative to the zero of energy used in the free-ion problem. The metallic eigenvalue E_k measured from the bottom of the band can, for present purposes, be replaced with its free-electron value. We then have

$$E_k' = E_0 + \tfrac{1}{2}k^2 - \langle \sum_{i \neq j} v_i + V_e \rangle, \tag{2.14}$$

where E_0 is the energy of the bottom of the conduction band and the last term is some suitable average of the neighbor core potentials and the electron potential inside the jth core. We have used the procedure proposed by Animalu and Heine[3] to evaluate E_k'. This procedure is not entirely adequate but it is nonetheless difficult to improve. The interactions between valence and core electrons are included implicitly in the calculation of E_0; this is the only place in the theory where these interactions enter. The calculation of E_k' is analogous to the calculation of core energies in pseudopotential theory and requires precisely the same approximations.

3. MODIFIED MODEL POTENTIAL

The model potential proposed by Heine and Abarenkov requires that we replace the ion-core potential with an $A_l(E)$ for all values of l from zero to infinity. As we have already emphasized, there is no direct way to determine the $A_l(E)$ for large angular momentum. In order to proceed, it was necessary to make an arbitrary and untenable assumption, namely, that for all $l>2$, $A_l(E) = A_2(E)$.

A point that seems to have been overlooked is that we can construct a weak model potential and a smooth model wave function without modeling the core potential for all l. Consider, for example, a metallic ion that has core states with angular quantum numbers $l \leq l_0$ and none with higher l [e.g., the highest core state in Al^{+3} is $2p$, so that $l_0=1$]. The lowest eigenstate for each $l>l_0$ will of course have no nodes at all and the higher states will have their nodes outside the core. Clearly, the $l>l_0$ components of a conduction-band wave function will be nodeless. As a consequence, there is nothing to be gained by modeling the core potential for $l>l_0$. These components of the wave function are already smooth and the effective potential is weak, so that we are justified in using perturbation theory.

Our first proposal for modifying the model potential is, then, to replace the core potential with an A_l only when there are core states with that l. For higher l we use the true potential. Clearly, this modification all but eliminates the problem of how to choose A_l for $l>2$, since there are very few simple metals with f core states. In fact, we shall frequently have to determine only A_0 and A_1, as with aluminum, and occasionally only A_0, as with lithium.

We make one further modification of the theory, that is, we allow the model radius $R_l(E)$ to depend on l and on energy. The motivation for this change will become clear when we optimize the potential. It appears that we may have complicated the problem somewhat by introducing a whole set of new parameters, the R_l. However, it is these new parameters that make the model potential flexible enough to optimize. We shall find, as might be expected, that optimizing the potential leads to a relation between the A_l and the R_l, so that, in fact, the number of parameters is not increased.

The new form of the bare model potential w_0 for a single ion can be written quite simply as

$$w_0 = v_b(r) - \sum_{l=0}^{l_0} \Theta(R_l - r)[A_l + v_b(r)]P_l, \tag{3.1}$$

$$\Theta(r) = 1, \quad r>0$$
$$= 0, \quad r<0$$

where $v_b(r)$ is the bare ion potential and l_0 is the largest angular quantum number for which there are core states. The model parameters A_l are still computed by assuming that $v_b(r) = -Z/r$ for $r>R_l$. Using this as-

sumption in (3.1) and regrouping terms somewhat, we obtain

$$w_0=-\frac{Z}{r}-\sum_{l=0}^{l_0}\Theta(R_l-r)\left(A_l-\frac{Z}{r}\right)P_l + \sum_{l=l_0+1}^{\infty}\Theta(R_C-r)v_{\text{core}}P_l. \quad (3.2)$$

The potential

$$v_{\text{core}}=v_b(r)+Z/r \quad (3.3)$$

is confined to the core region and arises from the neutral collection of nuclear charge $A-Z$ and core electrons. Note that the model radii for all $l>l_0$ are completely arbitrary and are in fact defined by the separation given in (3.2). For convenience we have chosen them all to be equal to the core radius R_C.

We expect the term in (3.2) involving $v_{\text{core}}(r)$ to make an extremely small contribution to the form factors for two related reasons. One is that the projection operator picks out components of the wave function with $l>l_0$. These components are extremely small near the ion center where $v_{\text{core}}(r)$ is large. Also, we know that for large l the core potential is dominated by the centrifugal term $l(l+1)/r^2$ at small r, so that the wave function is not altered by substantial changes in the details of $v_{\text{core}}(r)$.

To verify that this term actually is small, we have evaluated plane-wave matrix elements of it using Hartree-Fock potentials[14] and have found them to be at least two orders of magnitude smaller than the corresponding matrix elements of the term

$$-\sum_{l=0}^{l_0}\Theta(R_l-r)\left(A_l-\frac{Z}{r}\right)P_l$$

for all $q\leq 2k_F$. In view of these results we can accurately approximate the bare model potential by

$$w_0=-\frac{Z}{r}-\sum_{l=0}^{l_0}\Theta(R_l-r)\left(A_l-\frac{Z}{r}\right)P_l. \quad (3.4)$$

Though (3.4) is an approximation, we know precisely what effect we are neglecting when using it. Moreover, if we like, and if the core potentials are available, we can actually include the $v_{\text{core}}(r)$ term in the unscreened form factor.

4. OPTIMIZATION OF THE MODIFIED POTENTIAL

A. Cohen-Heine Variational Procedure

The modified model potential has a certain amount of inherent arbitrariness built in through the freedom in choosing $R_l(E)$. Though an optimization procedure formally eliminates this arbitrariness, it still remains in fact, because there is no rigorous criterion for optimization. Cohen and Heine[15] have suggested a reasonable criterion for optimization, that is, to seek the smoothest possible model wave function by minimizing

$$I=\int d^3r\,|\nabla\chi_k|^2\Big/\int d^3r\,\chi_k^*\chi_k. \quad (4.1)$$

We can rather easily transform (4.1) to a condition involving the total crystal model potential W. Integrating by parts once and using periodic boundary conditions to discard the surface term, we obtain

$$\int d^3r\,|\nabla\chi_k|^2=-\int d^3r\,\chi_k^*\nabla^2\chi_k = 2E_k\int d^3r\,\chi_k^*\chi_k-2\int d^3r\,\chi_k^*W\chi_k. \quad (4.2)$$

Therefore, minimizing (4.1) is equivalent to maximizing

$$I=\int d^3r\,\chi_k^*W\chi_k\Big/\int d^3r\,\chi_k^*\chi_k. \quad (4.3)$$

This condition seems to be rather unfortunate, because it appears to require a maximization of W. Yet we have repeatedly emphasized that the principal objective of the theory is to obtain a small W. In fact, Cohen and Heine suggested that an alternative optimization criterion might be minimization of (4.3). The confusion lies in the sign of W, which is negative. A second variation shows that (4.3) has only one stationary point, a maximum. Cohen and Heine claimed to be minimizing W but were actually maximizing a negative potential. In any event, there would be no need for concern, since W has been constrained to be small by determining $A_l(E)$ on the branch that gives a nodeless wave function. Any variation that we make to achieve the smoothest possible wave function will not alter W enough to invalidate the use of perturbation theory.

We now proceed to maximize (4.3), subject to variations in the model radii $R_l(E)$ at each ion site. The integrals in (4.3) extend over the whole crystal. Therefore we should, in principle, vary the $R_l(E)$ at every ion site simultaneously. However, since the model wave function around each ion site is dependent only on the R_l associated with that site and is completely independent of the R_l at all other sites, it is enough to maximize (4.3) subject to variations of the model radii at a single site. Varying model radii around stationary values $R_l^*(E)$ is essentially equivalent to varying wave functions around stationary solutions as done by Cohen and Heine[15] and by Harrison.[16] This is clear when we note that, since $\chi_k(\mathbf{r})$ is a function of the R_l, for small variations ΔR_l around the optimum radii we can write

$$\chi_k(R_l)=\chi_k(R_l^*+\Delta R_l)\cong\chi_k(R_l^*)+\sum_{l=0}^{l_0}\Delta R_l\left.\frac{\partial\chi_k}{\partial R_l}\right|_{R_l^*}. \quad (4.4)$$

[15] M. H. Cohen and V. Heine, Phys. Rev. **122**, 1821 (1961).

[16] W. A. Harrison, Ref. 5, Chap. 8.

The W appearing in (4.3) is the complete model potential for the crystal and includes the conduction-electron potential $V_e(\mathbf{r})$,

$$W(\mathbf{r})=V_e(\mathbf{r})+\sum_i w_0(\mathbf{r}-\mathbf{r}_i). \tag{4.5}$$

The bare model potential at a given ion site depends on the R_l at that site but is independent of all the other R_l. The electron potential is completely independent of the model radii.

Now, if we substitute (4.4) into (4.3) and note that each of the R_l at a single ion site is independent, we find that $I(R_l)$ is stationary, provided that

$$\frac{\partial}{\partial R_l}\frac{\langle\chi_k|W|\chi_k\rangle}{\langle\chi_k|\chi_k\rangle}\bigg|_{R_l^*}=0 \tag{4.6}$$

for all $l\leq l_0$. By making use of (4.5), Eq. (4.6) can be reduced to

$$\left[\frac{\partial}{\partial R_l}\langle\chi_k|V+w_0|\chi_k\rangle+I(R_l)\frac{\partial}{\partial R_l}\langle\chi_k|\chi_k\rangle\right]_{R_l=R_l^*}=0. \tag{4.7}$$

The integrals are now evaluated around one ion site but the condition (4.7) must hold independent of which site we choose.

It is appropriate to expand the model wave function in spherical components about an origin at the ion site where the R_l are being varied,

$$\chi_k(\mathbf{r})=\sum_{l,m}\frac{\chi_l(kr)}{r}Y_l^m(\theta,\varphi). \tag{4.8}$$

We may now write out (4.7) in detail,

$$\left\{\frac{\partial}{\partial R_l}\int_0^{R_l}dr\,\chi_l^*\chi_l[V_e(r)-A_l(R_l)]\right.$$
$$+\frac{\partial}{\partial R_l}\int_{R_l}^{\infty}dr\,\chi_l^*\chi_l[V_e(r)+v_b(r)]+I(R_l)$$
$$\left.\times\frac{\partial}{\partial R_l}\left(\int_0^{R_l}dr\,\chi_l^*\chi_l+\int_{R_l}^{\infty}dr\,\chi_l^*\chi_l\right)\right\}_{R_l=R_l^*}=0. \tag{4.9}$$

Next we recall that for $r<R_l$, the function $\chi_l(r)$ depends on R_l through the parameter $\gamma_l=[2(A_l+E)]^{1/2}$. This follows from Eq. (2.13). For $r>R_l$, the function $\chi_l(r)$ is independent of R_l. We use these results in (4.9) and immediately obtain

$$\left\{\frac{1}{\gamma_l}\frac{\partial A_l}{\partial R_l}\int_0^{R_l}dr\,[I(R_l)+A_l(R_l)-V_e(r)]\frac{\partial}{\partial\gamma_l}(\chi_l^*\chi_l)\right.$$
$$\left.+\frac{\partial A_l}{\partial R_l}\int dr\,\chi_l^*\chi_l+[A_l(R_l)+v_b(R_l)]\chi_l^*\chi_l\right\}_{R_l=R_l^*}=0. \tag{4.10}$$

We emphasize again that (4.10) holds for every $l\leq l_0$. For arbitrary energy this condition can be satisfied only if the conditions

$$A_l(R_l^*)=-v_b(R_l^*) \tag{4.11}$$

and

$$(\partial A_l/\partial R_l)\,|_{R_l^*}=0 \tag{4.12}$$

hold simultaneously.

It is not immediately obvious that this is the case. One of the two conditions can always be met by adjusting R_l. We must therefore show that this choice of R_l also implies the other. To do this we consider the logarithmic-derivative matching condition in a metal.

B. Equivalence of Optimization Conditions

We have shown that within the framework of the small-core approximation the logarithmic derivatives of exact and model wave functions are equal at the model radius,

$$L(R_l)\equiv\frac{1}{\chi_l(R_l)}\frac{d\chi_l}{dr}\bigg|_{R_l}=\frac{1}{\psi_l(R_l)}\frac{d\psi_l}{dr}\bigg|_{R_l}. \tag{4.13}$$

Equation (4.13) would also hold if we had chosen a slightly different model radius, $R_l'=R_l+\Delta R_l$. We take ΔR_l to be infinitesimal, so that

$$\frac{d}{dr}\psi_l(R_l+\Delta R_l)\cong\frac{d}{dr}\psi_l(R_l)+\Delta R_l\frac{d^2}{dr^2}\psi_l(R_l) \tag{4.14}$$

and

$$\psi_l(R_l+\Delta R_l)\cong\psi_l(R_l)+\Delta R_l\frac{d}{dr}\psi_l(R_l).$$

The expansions for χ_l and $d\chi_l/dr$ are slightly more complicated, since χ_l depends on γ_l, which depends on R_l. We find that

$$\frac{d}{dr}\chi_l(R_l+\Delta R_l)\cong\frac{d}{dr}\chi_l(R_l)+\Delta R_l\left[\frac{1}{\gamma_l^2}\frac{\partial A_l}{\partial R_l}\frac{d}{dr}\chi_l(R_l)\right.$$
$$\left.+\left(1+\frac{R_l}{\gamma_l^2}\frac{\partial A_l}{\partial R_l}\right)\frac{d^2}{dr^2}\chi_l(R_l)\right] \tag{4.15}$$

and

$$\chi_l(R_l+\Delta R_l)=\chi_l(R_l)+\Delta R_l\left(1+\frac{R_l}{\gamma_l^2}\frac{\partial A_l}{\partial R_l}\right)\frac{d}{dr}\chi_l(R_l).$$

Now we evaluate (4.13) at R_l', substitute the expansions (4.14) and (4.15), and use the Schrödinger equations (2.1) and (2.2) to eliminate $d^2\psi_l/dr^2$ and $d^2\chi_l/dr^2$. We find that the terms of order ΔR_l must be identically zero if the matching condition is to hold at both R_l and R_l'. From this requirement we obtain the expression

$$2[v_b(R_l)+A_l]+\frac{R_l}{\gamma_l^2}\frac{\partial A_l}{\partial R_l}\left\{L(R_l)\left[L(R_l)-\frac{1}{R_l}\right]\right.$$
$$\left.-\frac{l(l+1)}{R_l^2}+\gamma_l^2\right\}=0. \tag{4.16}$$

TABLE I. General optimized model potential parameters (in atomic units). The $A_l(E)$ for any element can be obtained directly by interpolating this table.

	$l=0$				$l=1$				$l=2$	
E/Z^2	ZR_l		A_l/Z^2		ZR_l		A_l/Z^2		ZR_l	A_l/Z^2
0.2958	1.450		0.6894							
0.2551	1.991		0.5020							
0.2222	2.532		0.3948							
0.1953	3.115		0.3210							
0.1730	3.735		0.2677							
0.1543	4.387		0.2279							
0.1385	5.083		0.1967							
0.1250	5.842		0.1712							
0.1133	6.628		0.1509		2.650		0.3773			
0.1033	7.421		0.1347		3.756		0.2662			
0.0945	8.298		0.1205		4.767		0.2097			
0.0868	9.196	2.066	0.1087	0.4840	5.809		0.1721			
0.0799	10.135	2.653	0.0987	0.3768	6.808		0.1469			
0.0739	11.151	3.296	0.0897	0.3033	7.805		0.1281			
0.0685	12.155	3.992	0.0823	0.2505	8.877		0.1126			
0.0637	13.236	4.766	0.0755	0.2098	9.954		0.1005			
0.0594	14.351	5.612	0.0697	0.1782	11.135		0.0898			
0.0555		6.517		0.1534	12.261		0.0816			
0.0520		7.496		0.1334	13.444	2.498	0.0744	0.4003	6.285	0.1591
0.0488		8.546		0.1170	14.706	3.587	0.0680	0.2788	8.192	0.1221
0.0459		9.644		0.1037		4.594		0.2176	9.873	0.1013
0.0432	2.087	10.864	0.4790	0.0920		5.657		0.1768	11.534	0.0867
0.0408	2.693	12.120	0.3712	0.0825		6.681		0.1497	13.070	0.0765
0.0385	3.365	13.437	0.2971	0.0744		7.728		0.1294	14.604	0.0685
0.0365	4.114	14.821	0.2431	0.0675		8.864		0.1128		
0.0346	4.956		0.2017			10.034		0.0997		
0.0328	5.898		0.1695			11.296		0.0885		
0.0312	6.936		0.1442			12.578		0.0795		
0.0297	8.074		0.1239		2.475	13.940	0.4039	0.0717	5.852	0.1709
0.0283	9.313		0.1074		3.533		0.2830		7.621	0.1312
0.0270					4.544		0.2200		9.259	0.1080

We are always free to choose $R_l=R_l^*$ such that $A_l(R_l^*)=-v_b(R_l^*)$. If we make this choice, then it follows immediately from (4.16) that

$$(\partial A_l/\partial R_l)\,|_{R_l^*}=0$$

as well. That is, the two conditions (4.11) and (4.12) are equivalent. Therefore, to optimize the potential, we simply select the model radii that allow us to match the model potential smoothly to $v_b(r)$ for each $l\leq l_0$.

This optimization condition is actually almost an obvious one. We might expect that eliminating discontinuities in the potential would tend to decrease any oscillations in the model-potential form factors at short wavelengths. As we have already remarked, Animalu and Heine[3] did notice that such oscillations were reduced if $A_l(E)$ was chosen roughly equal to Z/R_M. However, in their formulation it was impossible to achieve perfect matching for all l. Of course, there still are discontinuities in the derivatives of the potential at R_l that give rise to small form-factor oscillations at large q. If we had elected to construct a well varying linearly with r, for example, we could presumably eliminate not only the potential discontinuity, but also the first-derivative discontinuity. Further discontinuities could be eliminated by including higher powers of r in the model potential. If this procedure were carried to the limit, we would find that we had simply constructed the Taylor series for the exact potential. One finds that attempting to construct model potentials more complicated than the simple square well introduces sufficient complications that the method is no longer practical.

C. Internal Consistency

At this point in our discussion it is worthwhile to summarize the key constraints that we have imposed in constructing the optimum model potential: (i) The core potential is modeled only for $l\leq l_0$, where l_0 is the maximum angular momentum of core states; (ii) the model parameters $A_l(E)$ have been selected to give model wave functions $\chi_l(r)$ that have no nodes in the core; and (iii) optimization requires that $A_l=-v_b(R_l)$. Of these constraints, only the second can be regarded as a fundamental requirement of the theory. Initially, each constraint was established independent of the others. For instance, in deriving the optimization condition we did not have to specify a range of l or that the model wave function be nodeless. However, when imposed simultaneously, these constraints are no longer independent.

To show this we apply the Wronskian theorem[13] to the Schrödinger equations

$$\frac{d^2\psi_l(r)}{dr^2}-\left[\frac{l(l+1)}{r^2}+2v_b(r)+2V_e(r)-2E\right]\psi_l(r)=0 \quad (4.17)$$

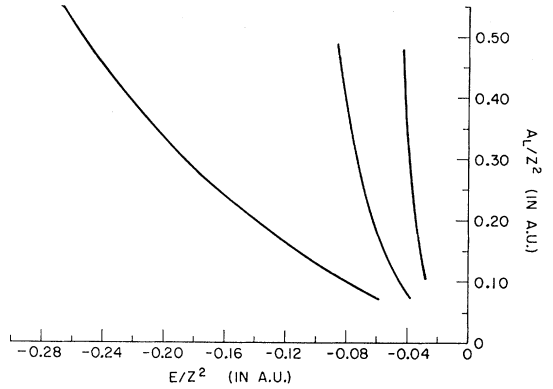

FIG. 7. Optimized model-potential parameters versus energy for $l=0$. These curves can be used to obtain $A_l(E_F)$ directly by doing the linear extrapolation graphically.

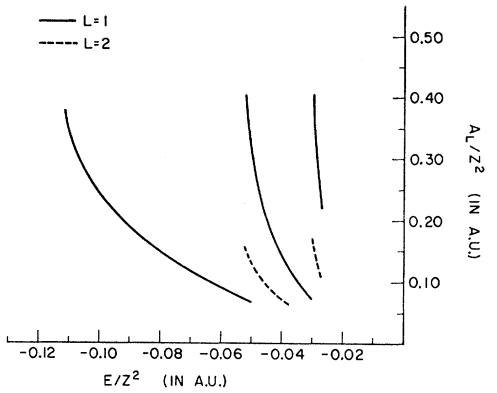

FIG. 8. Optimized model-potential parameters versus energy for $l=1, 2$.

and

$$\frac{d^2\chi_l}{dr^2}-\left[\frac{l(l+1)}{r^2}-2A_l+2V_e(r)-2E\right]\chi_l(r)=0. \quad (4.18)$$

Since the logarithmic derivatives of $\psi_l(r)$ and $\chi_l(r)$ have been matched in determining $A_l(E)$, independent of what R_l we pick, the boundary terms vanish and we are left with

$$\int_0^{R_l} dr\,[A_l(R_l)+v_b(r)]\psi_l(r)\chi_l(r)=0. \quad (4.19)$$

Now, suppose that we require a nodeless $\chi_l(r)$ but relax the constraint that limits the model potential to $l\leq l_0$. For $l>l_0$ we have seen that $\psi_l(r)$ is nodeless in the core. Therefore (4.19) cannot hold unless $A_l+v_b(r)$ changes sign in the range of integration, which precludes having $A_l=-v_b(R_l)$. We conclude that, had we not constrained l to be less than l_0, we would have encountered an inconsistency in trying to optimize the potential.

It is important to emphasize that we have achieved internal consistency only in the sense that, having required the first constraint, we have avoided contradicting the Wronskian theorem. We have not proved that our three constraints are necessarily consistent. However, empirically we have found no apparent difficulties in obtaining optimum model parameters for the modified model potential.

D. Optimized Model-Potential Parameters

Model-potential parameters are calculated by assuming that $v_b(r)=-Z/r$ outside of the model radius. The optimization condition is then simply

$$A_l=Z/R_l. \quad (4.20)$$

We can obtain optimized parameters by interpolating Abarenkov's[12] tables to find A_l that satisfy (4.20). A program has been written to carry out this interpolation. The accuracy of the results is limited somewhat by the fact that Abarenkov evaluated A_l at widely spaced values of R_M. However, the figures are probably accurate to two decimal places, which is really all the accuracy required in view of the crude A_l-versus-E extrapolation that must be made.

The optimized model parameters are listed in Table I and plotted in Figs. 7 and 8. The parameters for any element can be obtained from this table using the appropriate Z and the ionic-term values. To determine A_l at the Fermi energy it is necessary to extrapolate linearly, as discussed in Sec. 2. We have done this for a series of elements and listed the parameters in Table II.

TABLE II. Optimized model-potential parameters (in atomic units) evaluated at the Fermi energy. These figures can be regarded as accurate to at least two decimal places.

Element	$R_0(E_F)$	$A_0(E_F)$	$\partial A_0/\partial E$	$R_1(E_F)$	$A_1(E_F)$	$\partial A_1/\partial E$	$R_2(E_F)$	$A_2(E_F)$	$\partial A_2/\partial E$
Li	3.02	0.331	−0.186						
Be	2.00	1.000	−0.202						
Na	3.26	0.307	−0.231	2.71	0.369	−0.196			
Mg	2.58	0.776	−0.286	2.19	0.912	−0.058			
Al	2.15	1.395	−0.326	1.82	1.647	−0.044			
K	4.20	0.238	−0.294	4.00	0.250	−0.120			
Rb	4.46	0.224	−0.336	4.48	0.223	−0.159	[a]	[a]	[a]
Zn	2.03	0.984	−0.355	1.45	1.380	−0.484	2.33	0.860[b]	0
Cd	2.24	0.892	−0.424	1.75	1.144	−0.513	2.16	0.924[b]	−0.571
In	2.24	1.341	−0.454	2.01	1.494	−0.224	2.75	1.089	+0.094

[a] No values are obtainable using the range of parameters in Abarenkov's tables.
[b] Obtained by extrapolation beyond the range of Abarenkov's tables.

TABLE III. Depletion holes evaluated using the optimized model potential. OPW orthogonalization holes are given for comparison.

Element	$-\rho/Z$	$-\rho^{\mathrm{OPW}}/Z$
Li	0.08367	0.068
Be	0.06218	0.057
Na	0.08923	0.074
K	0.12533	0.144
Mg	0.07568	0.079
Al	0.06564	0.076
Rb	0.14569[a]	
Zn	0.07306	0.138
Cd	0.08629	
In	0.07225	

[a] Computed without $l=2$ terms.

It is worth noting that the values of $A_l(E_F)$ and the corresponding $R_l(E_F)$ do not differ much from those given by Animalu.[16] However, the difference is enough to make significant changes in the form factors.

5. NUMERICAL RESULTS

The general expressions for the screened form factor and the depletion hole given recently by Shaw and Harrison[17] hold without modification for the new optimized model potential. However, the details of the expressions used for computation must be altered somewhat.

We look first at the depletion hole[17]

$$\rho=-\sum_{k\leq k_F}\int_{\Omega_M} d^3r\,\chi_k^*(\mathbf{r})\frac{\partial w}{\partial E_k}\chi_k(\mathbf{r}). \tag{5.1}$$

The derivation of this expression does not depend on the detailed structure of the model potential w and is therefore valid for the optimum potential

$$w=V_e(r)+v_b(r)-\sum_{l=0}^{l_0}\Theta(R_l-r)[A_l+v_b(r)]P_l. \tag{5.2}$$

We need only require that $\Omega_M>\frac{4}{3}\pi R_l^3$ for every l. To obtain an explicit expression for ρ we differentiate (5.2), recalling that $R_l(E)$ is now a function of energy:

$$\frac{\partial w}{\partial E}=-\sum_{l=0}^{l_0}\delta(R_l-r)\frac{\partial R_l}{\partial E}[A_l+v_b(r)]P_l - \sum_{l=0}^{l_0}\frac{\partial A_l}{\partial E}\Theta(R_l-r)P_l. \tag{5.3}$$

For the optimized model potential $A_l=-v_b(R_l)$, so that the first term in (5.3) vanishes. Therefore, to lowest order in w, the depletion hole is

$$\rho=-\frac{4}{\pi}\sum_{l=0}^{l_0}(2l+1)\frac{\partial A_l}{\partial E}\int_0^1 dx\,x^2\int_0^1 dy \times y^2k_F{}^3R_l{}^3(x)j_l{}^2[k_FR_l(x)xy]. \tag{5.4}$$

[17] R. W. Shaw, Jr., and W. A. Harrison, Phys. Rev. **163**, 604 (1967).

This expression differs from the one used previously to compute ρ, in that it accounts for the energy dependence of $R_l(E)$ in integrating over $\mathbf{k}$ and the sum over l goes only to l_0. These differences are sufficient to alter the values of ρ given by Shaw and Harrison. We have computed new depletion holes for a group of elements. The results are given in Table III and compared with orthogonalized-plane-wave (OPW) orthogonalization holes.[5] It is interesting to note that the depletion hole for beryllium, which was previously found to be negative,[17] becomes positive when calculated with the new potential.

We have computed form factors using the approximate bare model potential given in Eq. (3.4). The errors inherent in neglecting the $v_{\mathrm{core}}(r)$ term in (3.2) are insignificant compared with the inaccuracies in the $A_l(E)$. From (3.4) the local and nonlocal contributions to the unscreened form factor are[18]

$$v_q=-4\pi Z/q^2\Omega_0 \tag{5.5}$$

and

$$f(\mathbf{k},\mathbf{q})=-\frac{4\pi}{\Omega_0}\sum_{l=0}^{l_0}(2l+1)P_l(\cos\theta)A_lR_l{}^3\int_0^1 dx \times x(x-1)j_l(k'R_lx)j_l(kR_lx), \tag{5.6}$$

where Ω_0 is the atomic volume Ω/N.

The screened form factor is calculated exactly as in Shaw and Harrison. A program has been written to evaluate these form factors, as well as band-structure energies and effective interactions between ions, for the optimum model potential.[19] The form factors for a group of eight elements are given in Table IV. There are several interesting features of these results that we should mention. The form factors tend to be somewhat smaller than the previous model-potential or pseudopotential results in the region of the first few reciprocal-lattice vectors. In addition, the optimized form factors decay more rapidly than those of Animalu[16] at short wavelengths. The small oscillations that remain are due to discontinuities in the derivatives of the potential at $R_l(E)$. Finally, we note the dip in the indium and cadmium ($l_0=2$) form factors below $q=2k_F$. This is not a spurious effect, but arises from the $l=2$ contribution to the nonlocal part of the form factor.

Note that the model-potential form factor is nonlocal, that is, it depends not only on the scattering momentum q, but also on the initial-state wave number k and on the scattering angle. The results given in Table IV are computed for scattering on the Fermi surface when $q\leq 2k_F$ and for backscattering when $q>2k_F$. To illustrate the k dependence of the form factor, we have

[18] See Ref. 17 for notation.

[19] A report containing a complete listing and discussion of the program used in these computations is available on request, from Reports Office, W. W. Hansen Laboratories, Stanford University, Stanford, Calif. 94305 (unpublished).

plotted in Fig. 9 the indium form factor computed for scattering on various energy shells. In Fig. 10, we have plotted the indium form factor as a function of scattering angle for two scattering momenta and an initial-state momentum of $k=\frac{1}{2}k_F$. The table included in the figure gives the corresponding form factors for energy-shell and Fermi-surface scattering. It is evident that the value of the nonlocal form factor can differ from $\omega_q(k_F)$ by up to an order of magnitude. In calculations of metallic properties it is important to include correctly the full nonlocal model potential.

We have plotted the optimized form factor for aluminum in Fig. 11 and have compared it with Animalu's[16] results. The comparison is not really relevant, since the form factors given by Animalu were computed using a potential which was not internally consistent.[17] We should emphasize that both the reformulation of the model potential discussed earlier[17] and the modifications and optimization given here are based on first-principles arguments and do not represent an attempt to obtain agreement with experimental results. It is now important to determine how well the reformulated

TABLE IV. Form factors for eight metals evaluated using the optimized model potential. $w_q^{\rm opt}(k_F)$ is in atomic units. For $q<2k_F$ these results describe scattering on the Fermi surface; for $q>2k_F$ they describe backscattering.

q/k_F	Li	Be	Na	Mg	Al	K	Cd	In
0	−0.11564	−0.35274	−0.07945	−0.17482	−0.28664	−0.05193	−0.18367	−0.21184
0.1	−0.11374	−0.34631	−0.07815	−0.17185	−0.28144	−0.05091	−0.17929	−0.20779
0.2	−0.11111	−0.33403	−0.07662	−0.16688	−0.27152	−0.04996	−0.17469	−0.20156
0.3	−0.10686	−0.31470	−0.07415	−0.15895	−0.25587	−0.04840	−0.16730	−0.19169
0.4	−0.10117	−0.28976	−0.07081	−0.14851	−0.23562	−0.04630	−0.15757	−0.17886
0.5	−0.09428	−0.26086	−0.06674	−0.13612	−0.21210	−0.04373	−0.14601	−0.16386
0.6	−0.08641	−0.22960	−0.06206	−0.12236	−0.18664	−0.04076	−0.13316	−0.14753
0.7	−0.07783	−0.19740	−0.05694	−0.10783	−0.16045	−0.03748	−0.11955	−0.13062
0.8	−0.06878	−0.16541	−0.05150	−0.09304	−0.13454	−0.03398	−0.10565	−0.11378
0.9	−0.05948	−0.13444	−0.04588	−0.07844	−0.10970	−0.03036	−0.09182	−0.09752
1.0	−0.05012	−0.10506	−0.04022	−0.06437	−0.08647	−0.02670	−0.07839	−0.08218
1.1	−0.04084	−0.07758	−0.03460	−0.05110	−0.06520	−0.02308	−0.06555	−0.06795
1.2	−0.03176	−0.05215	−0.02913	−0.03882	−0.04611	−0.01956	−0.05346	−0.05490
1.3	−0.02297	−0.02879	−0.02387	−0.02764	−0.02926	−0.01621	−0.04218	−0.04300
1.4	−0.01452	−0.00744	−0.01888	−0.01763	−0.01465	−0.01309	−0.03174	−0.03212
1.5	−0.00646	0.01202	−0.01420	−0.00881	−0.00222	−0.01022	−0.02213	−0.02208
1.6	0.00122	0.02974	−0.00986	−0.00117	0.00813	−0.00765	−0.01330	−0.01264
1.7	0.00851	0.04589	−0.00586	0.00531	0.01651	−0.00540	−0.00518	−0.00352
1.8	0.01546	0.06066	−0.00222	0.01070	0.02306	−0.00349	0.00231	0.00562
1.9	0.02212	0.07430	0.00107	0.01506	0.02794	−0.00193	0.00930	0.01512
2.0	0.02880	0.08742	0.00410	0.01859	0.03145	−0.00072	0.01603	0.02554
2.1	0.03228	0.09152	0.00628	0.02038	0.03243	0.00043	0.01993	0.02997
2.2	0.03467	0.09321	0.00798	0.02109	0.03191	0.00129	0.02287	0.03327
2.3	0.03628	0.09327	0.00923	0.02098	0.03032	0.00187	0.02500	0.03557
2.4	0.03721	0.09199	0.01008	0.02020	0.02792	0.00217	0.02642	0.03723
2.5	0.03755	0.08964	0.01056	0.01888	0.02490	0.00223	0.02722	0.03809
2.6	0.03740	0.08643	0.01071	0.01715	0.02145	0.00209	0.02748	0.03831
2.7	0.03683	0.08256	0.01059	0.01510	0.01772	0.00178	0.02729	0.03790
2.8	0.03591	0.07819	0.01024	0.01285	0.01386	0.00134	0.02673	0.03716
2.9	0.03470	0.07347	0.00970	0.01047	0.00997	0.00081	0.02585	0.03586
3.0	0.03327	0.06852	0.00900	0.00803	0.00615	0.00021	0.02471	0.03431
3.1	0.03166	0.06346	0.00819	0.00561	0.00249	−0.00042	0.02338	0.03239
3.2	0.02992	0.05838	0.00729	0.00324	−0.00095	−0.00108	0.02189	0.03022
3.3	0.02810	0.05336	0.00633	0.00098	−0.00410	−0.00172	0.02030	0.02784
3.4	0.02622	0.04848	0.00534	−0.00114	−0.00695	−0.00235	0.01863	0.02531
3.5	0.02432	0.04379	0.00433	−0.00309	−0.00944	−0.00294	0.01691	0.02267
3.6	0.02243	0.03934	0.00333	−0.00485	−0.01157	−0.00348	0.01519	0.01997
3.7	0.02057	0.03515	0.00234	−0.00640	−0.01333	−0.00396	0.01348	0.01726
3.8	0.01876	0.03127	0.00140	−0.00772	−0.01471	−0.00438	0.01180	0.01457
3.9	0.01702	0.02770	0.00049	−0.00883	−0.01572	−0.00474	0.01017	0.01194
4.0	0.01537	0.02446	−0.00035	−0.00971	−0.01638	−0.00503	0.00861	0.00942
4.1	0.01380	0.02154	−0.00113	−0.01037	−0.01672	−0.00524	0.00712	0.00702
4.2	0.01234	0.01895	−0.00184	−0.01082	−0.01674	−0.00539	0.00573	0.00479
4.3	0.01099	0.01667	−0.00248	−0.01107	−0.01648	−0.00547	0.00444	0.00275
4.4	0.00975	0.01468	−0.00304	−0.01113	−0.01598	−0.00548	0.00325	0.00091
4.5	0.00862	0.01297	−0.00352	−0.01101	−0.01527	−0.00543	0.00217	−0.00070
4.6	0.00760	0.01152	−0.00393	−0.01075	−0.01438	−0.00533	0.00119	−0.00208
4.7	0.00669	0.01030	−0.00425	−0.01035	−0.01335	−0.00518	0.00033	−0.00322
4.8	0.00589	0.00930	−0.00450	−0.00983	−0.01221	−0.00498	−0.00043	−0.00412
4.9	0.00519	0.00847	−0.00468	−0.00922	−0.01099	−0.00474	−0.00107	−0.00478
5.0	0.00458	0.00781	−0.00478	−0.00853	−0.00974	−0.00447	−0.00162	−0.00522
5.4	0.00297	0.00627	−0.00460	−0.00541	−0.00487	−0.00320	−0.00287	−0.00504
5.8	0.00230	0.00558	−0.00373	−0.00247	−0.00120	−0.00191	−0.00294	−0.00284
6.2	0.00209	0.00495	−0.00254	−0.00041	0.00068	−0.00087	−0.00230	−0.00020
6.6	0.00200	0.00413	−0.00137	0.00057	0.00094	−0.00022	−0.00137	0.00160
7.0	0.00184	0.00322	−0.00044	0.00061	0.00023	0.00002	−0.00048	0.00204

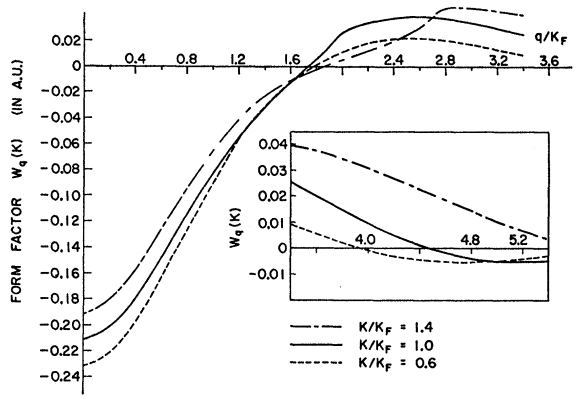

FIG. 9. Optimized model-potential form factors for indium calculated for scattering on various energy shells.

model-potential theory can predict various experimental observations.

We have used the optimized model potential in two calculations of metallic properties. The energy-wave-

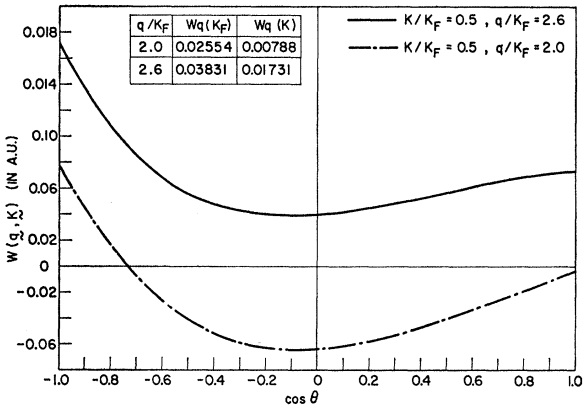

FIG. 10. Indium form factor as a function of scattering angle for two scattering momenta.

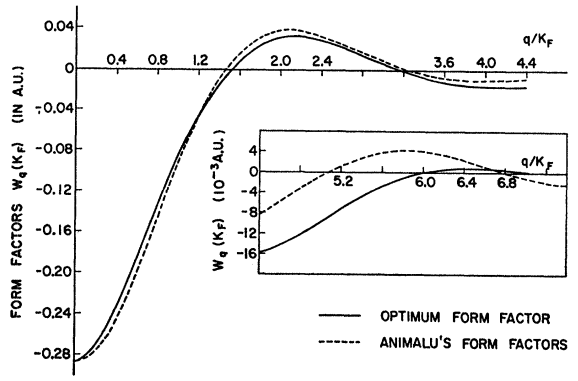

FIG. 11. Optimized model-potential form factor for aluminum. The form factor obtained by Animalu is given for comparison. These form factors are obtained by taking $|k|=|k+q|=k_F$ for $q\leq 2k_F$ and $k+q$ antiparallel to k for $q>2k_F$.

number characteristics[5] have been computed for a group of simple metals and the results have been used to evaluate the band-structure energy and thereby to determine stable crystal structures for these metals. The details of this work will be reported in a separate paper. We have also studied the properties of liquid metals using the optimized model potential.[20] A paper on this work is forthcoming.

ACKNOWLEDGMENTS

The author would like to express his gratitude to Professor Walter A. Harrison, who has been a constant source of encouragement and stimulation. Thanks are also due to Dr. A. O. E. Animalu for his continued interest in this work.

[20] R. W. Shaw, Jr., and N. V. Smith, Phys. Rev. (to be published).